ELSEVIER

Journal of Molecular Structure (Theochem) 335 (1995) 181–188

THEO
CHEM

Computer simulation of solvation dynamics in hydrogen-bonding liquids

Munir S. Skaf*[,1], Branka M. Ladanyi

Department of Chemistry, Colorado State University, Fort Collins, CO 80523, USA

Received 26 December 1993; accepted 6 June 1994

Abstract

The dynamics of solvation following an instantaneous reversal of the dipole moment, $(e/2, -e/2) \rightarrow (-e/2, e/2)$, of diatomic solutes immersed in methanol–water mixtures is investigated through molecular dynamics simulations. We study the solvation response functions for two different solute sizes in an equimolar methanol–water mixture and compare them with the corresponding responses in pure methanol. The total response functions for the mixture are separated into methanol and water contributions in order to identify methanol- and water-like features of the response. Several equilibrium solute–solvent site–site pair distribution functions are also calculated to help elucidate the effects of the solute size on the solvation response.

1. Introduction

Chemical reactions of charged or polar species, such as those participating in electron and proton transfers, are strongly affected by the presence of polar solvents. Solvent effects on these reactions have long been a subject of intense research activity in chemistry and biochemistry [1–5]. More recently, attention has turned to the dynamic solvent effects, i.e. the time scale of the solvent's response to the change in the solute charge distribution. In intramolecular electron transfer reactions, this step is often rate determining [3–5]. Solvation dynamics on the subpicosecond time scale has recently become experimentally accessible through time-resolved measurements in the Stokes shift in the fluorescence spectrum of dissolved probe molecules [6,7]. Considerable efforts have been directed toward developing a microscopic, molecular level understanding of the solvent relaxation mechanisms observed in these experiments and much progress has been made (see, for instance, Ref. [7] and references therein).

Molecular dynamics (MD) simulations have been used with great success in the study of solvation dynamics in polar liquids. Numerous simulations [7–18] have been carried out on several solute–solvent systems undergoing different excitations, i.e. solute ground- to excited-state perturbations, under different thermodynamic conditions. Despite the fact that most MD simulations of solvation dynamics user simpler model solutes than the complex chromophores used in time-dependent Stokes shift experiments, many new

---

* Corresponding author.

[1] Present address: Departamento de Quimica, FFCLRP — Universidade de Sao Paulo, Av. Bandeirantes, 3900 Ribeirão Preto, SP 14040-901, Brazil

SSDI 0166-1280(94)03999-2

aspects of the problem have been understood by means of computer simulations. In particular, MD simulations have revealed the relative importance of inertial relaxation at the earliest stages of solvation dynamics in fluids such as methanol [14,19], water [9,19] and acetonitrile [13,19]. Direct experimental evidence of an initial inertial component to the solvation dynamics has been reported [19] for methanol and acetonitrile in good agreement with simulation results.

While the rate of decay of the inertial contributions to the solvation response function at short times depends essentially on the magnitudes of the solvent molecular moments of inertia [14,15,19], the subsequent, post-inertial decay is strongly dependent on the solvent's degree of association and on the rate of formation of solute–solvent hydrogen (H) bonds [15,16,20]. These, in turn affect the relative importance of inertial decay to the total solvation response [15]. In methanol [14–17,19] and water [8–10,18], the two H-bonding liquids studied by MD, the solvation response functions also exhibit rapid oscillatory motion due to H-bond (O···H–O) libration. Despite these common features, the solvation responses of methanol and water are quantitatively very different from each other because the relative importance of the inertial decay, the subsequent librational regime, and the slow diffusional relaxation are different in these solvents [14,15]. Specifically, methanol exhibits a smaller inertial decay regime, less prominent oscillatory behavior, and larger contributions from diffusional dynamics than water does. The difference in the relative importance of inertial decay can be ascribed to the fact that all of water's moments of inertia are small, since they depend predominantly on masses of the hydrogens, while in methanol only one out of three moments of inertia is small. The librational and diffusional regimes are likely to depend on the connectivity, strength and persistence of the H-bond network. However, an explicit connection between solvation dynamics in H-bonding liquids and these properties of the H-bond network has not yet been established.

In view of the differences of the solvation dynamics exhibited by water and methanol, their importance as reaction media, and given the fact that the structural, dynamic, and H-bonding properties of these solvents change upon mixing [21,22], it is interesting to investigate the solvation dynamics in methanol–water mixtures, exploring, as much as possible, the separate contributions from both moieties to the total response. With this aim, we have performed a series of MD simulations of the solvation dynamics in methanol–water mixtures of different compositions using different types of probe solute molecules. In this article, we report a preliminary account of the results of these simulations, focusing on equimolar mixtures. We report solvation responses following a sudden reversal (or flip) of the dipole moments of diatomic solutes of different sizes and compare the results with those obtained by Fonseca and Ladanyi for pure methanol [15]. Solute–solvent pair distribution functions are also calculated in order to aid our analyses of the solvation responses.

2. Solvation response and computational details

In time-dependent Stokes shift experiments, the most commonly reported quantity is the normalized response function of the frequency, $\nu(t)$, at the maximum of the fluorescence band [1–7]:

$$C(t) = \frac{h\nu(t) - h\nu(\infty)}{h\nu(0) - h\nu(\infty)} \tag{1}$$

where the electronic excitation occurs at time $t = 0$, and $t = \infty$ corresponds to the time at which equilibrium solvation of the excited state solute has been reached. In MD simulations, the solvation response function $C(t)$ is obtained by monitoring the time evolution of the energy difference ΔE between the solute–solvent interaction energies for the ground (G) and excited (E) electronic states [11]. In our case, where the electronic excitation means just an internal redistribution of the solute atomic charges, ΔE is given by the electrostatic solute–solvent interactions:

$$\Delta E = U_{\mathrm{el}}^{\mathrm{E}} - U_{\mathrm{el}}^{\mathrm{G}} \tag{2}$$

where $U_{\mathrm{el}}^{\mathrm{E}}$ and $U_{\mathrm{el}}^{\mathrm{G}}$ are the excited- and ground-state solute–solvent electrostatic potential energies which are readily obtained in the course of the simulation. The response function is then

Table 1
Site parameters for the diatomic solutes used in the simulations. The site–site separation is 1.40 Å for both solute types

Solute	$\epsilon_{\alpha\alpha}/k_B$ (K)	$\sigma_{\alpha\alpha}$ (Å)	q_α (e)	m_α (a.u.)
Small	87.9	3.083	±0.5	30
Large	87.9	4.20	±0.5	30

calculated from

$$C(t) = \frac{\overline{\Delta E(t)} - \overline{\Delta E(\infty)}}{\overline{\Delta E(0)} - \overline{\Delta E(\infty)}} \tag{3}$$

where the overbar indicates an average over nonequilbrium trajectories. The system is equilibrated in the presence of the ground state solute, whose charge distribution is instantaneously changed at $t = 0$, and the trajectory is then propagated in the presence of this new distribution. The sudden change in the charge distribution corresponds to the solute electronic transition which according to the Franck–Condon principle, happens essentially instantaneously on the time-scale of nuclear motions. In order to gain access to the dynamic effects of the methanol and water molecules separately, we have calculated ΔE in terms of the solute–methanol, ΔE_M, and solute–water, ΔE_W, interaction energies. The normalized total response function reads then

$$C(t) = C_M(t) + C_W(t) \tag{4}$$

where

$$C_M(t) = \frac{\overline{\Delta E_M(t)} - \overline{\Delta E_M(\infty)}}{\overline{\Delta E(0)} - \overline{\Delta E(\infty)}} \tag{5a}$$

and

$$C_W(t) = \frac{\overline{\Delta E_W(t)} - \overline{\Delta E_W(\infty)}}{\overline{\Delta E(0)} - \overline{\Delta E(\infty)}} \tag{5b}$$

We have simulated dipole flips $(-e/2, e/2) \rightarrow (e/2, -e/2)$ in diatomic solutes in which the two sites differ only by their partial charges ($\pm e/2$), immersed in an equimolar methanol–water mixture. We have considered two different sizes of solute molecules whose site interaction potentials are given by Lennard-Jones plus Coulomb terms:

$$u_{\alpha\beta}(r) = 4\epsilon_{\alpha\beta}\left[\left(\frac{\sigma_{\alpha\beta}}{r}\right)^{12} - \left(\frac{\sigma_{\alpha\beta}}{r}\right)^{6}\right] + \frac{q_\alpha q_\beta}{4\pi\epsilon_0 r} \tag{6}$$

The solute site Lennard-Jones potential parameters, $\epsilon_{\alpha\alpha}$ and $\sigma_{\alpha\alpha}$, partial charges, q_α, and masses, m_α, are given in Table 1. We refer to the solutes as "small" ($\sigma_{\alpha\alpha} = 3.083$ Å) and "large" ($\sigma_{\alpha\alpha} = 4.20$ Å). The small solute site diameters are the same as those of solvent oxygens, while the large site diameter exceeds the size of the methyl group. The solute molecular bond length is fixed at 1.40 Å. The model used for methanol is the H1 [23] and for water for TIP4P [24]. Both are described by the site–site potentials of Eq. (6). The corresponding site parameters and molecular geometries may be found in Ref. [22]. The Lennard-Jones interaction parameters between unlike sites have been evaluated via the usual Lorentz–Berthelot combining rules (see, for instance, Ref. [26]).

The simulated equimolar mixture consists of 500 particles (250 methanol molecules, 249 water and one solute) in a box, whose dimensions ($L = 28.66$ Å) correspond to the experimental density of an equimolar methanol–water mixture at 298 K and atmospheric pressure. The simulations were performed in the NVE ensemble using the generalized method of constraints [25] to keep the molecular geometries fixed and the leap-frog algorithm (see, for instance, Ref. [26]) to integrate the equations of motion with a time step of 4 fs. Periodic boundary conditions and $\frac{1}{2}$ box length cutoff were applied to Lennard-Jones interactions while the long-range forces were handled by the Ewald summation technique [26]. The nonequilibrium simulations were performed as follows. First, a set of statistically independent initial configurations was extracted from equilibrium trajectories of the mixture with the solute in its ground state. Then, an instantaneous switch of the solute's atomic charges was performed and the system was allowed to relax to equilibrium. During this process, the energy differences ΔE_M and ΔE_W were recorded for later analysis. About 240 independent trajectories of 1.2 ps duration were recorded for each solute type and used to calculate the average ΔE values entering Eqs. (4) and (5).

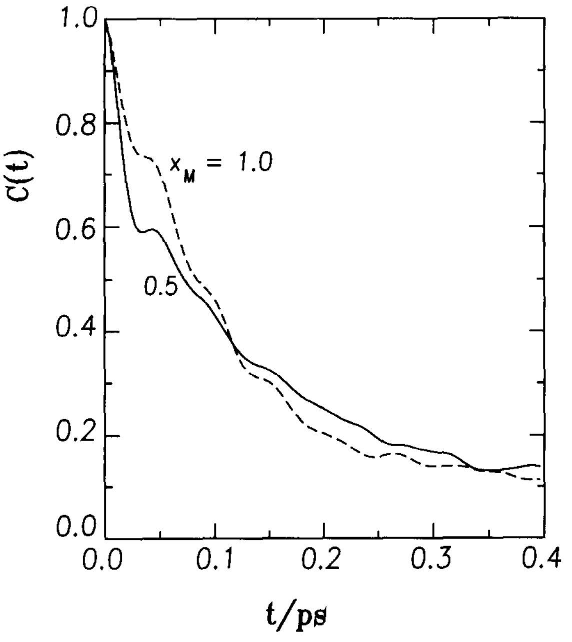

Fig. 1. Non-equilibrium response functions for a dipole flip $(e/2, -e/2) \rightarrow (-e/2, e/2)$, of the large solute in an equimolar methanol–water mixture (solid line) and pure methanol (broken line) [15].

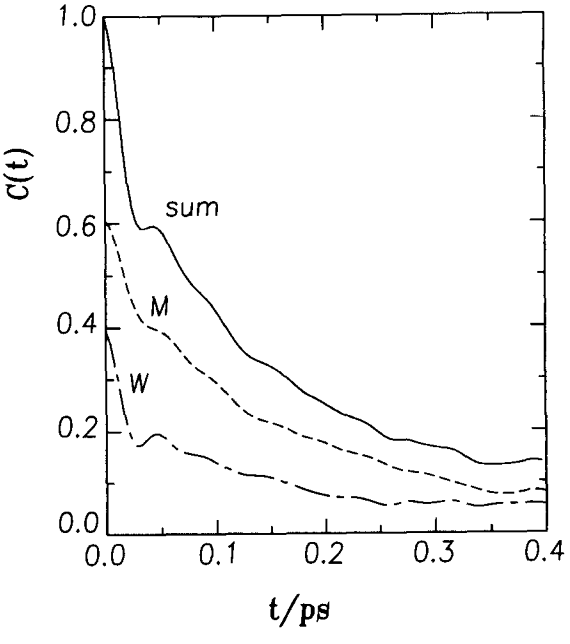

Fig. 2. Total response function for large solute in the equimolar mixture (solid line) and its contributors, $C_M(t)$ (broken line) and $C_W(t)$ (long and short dashes) from solute–methanol and solute–water interaction energies.

3. Results and discussion

We begin our discussion by showing in Fig. 1 the nonequilibrium normalized response functions $C(t)$ for a dipole flip of the large solute in the equimolar mixture and the corresponding function for pure methanol, obtained by Fonseca and Ladanyi [15]. The most conspicuous features of both curves are their overall nonexponential shapes, and the fact that the responses are about 90% relaxed within a time scale of a few hundreds of femtoseconds. In the early stages of solvation in methanol (from 0 to 20 fs), the decay is essentially inertial or Gaussian and is dominated by the free rotation of the hydroxy hydrogen around the C–O axis, as shown elsewhere [14,15]. During roughly the same time interval the mixture's response exhibits a faster decay due to the presence of the lighter (in terms of moments of inertia) water molecules surrounding the solute. The librational oscillations, occurring in mainly the 20–80 fs time interval, are also more pronounced in the mixture than in pure methanol. This is due to the fact that water molecules form, on average, a larger number of H-bonds than methanol [20,21] and their presence thus enhances the amplitude of librational oscillations. An interesting feature of the mixture's response shown in Fig. 1 is the fact that it resembles that of pure methanol at longer times, and actually relaxes somewhat more slowly. This is consistent with the MD analysis of the dynamics of methanol–water mixtures carried out by Ferrario et al. [22], who show that water–water and water–methanol H-bonds have longer lifetimes in the equimolar mixture than in pure methanol, and that methanol has longer reorientational times when water is added to the system.

The separate contributions from methanol, $C_M(t)$, and water, $C_W(t)$, to the total response for the large solute are displayed in Fig. 2. There, it can be noticed that $C_W(t)$ exhibits more pronounced librational oscillations than $C_M(t)$, being able, therefore, to sustain a relatively higher degree of correlations in the time interval (20–80 fs) due to the water molecules' better efficiency at hindering the inertial rotations by means of their H-bond

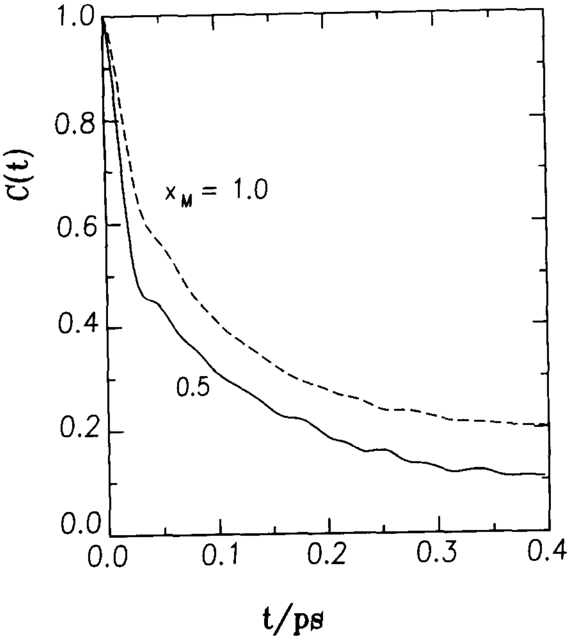

Fig. 3. Same as Fig. 1, but for the small solute.

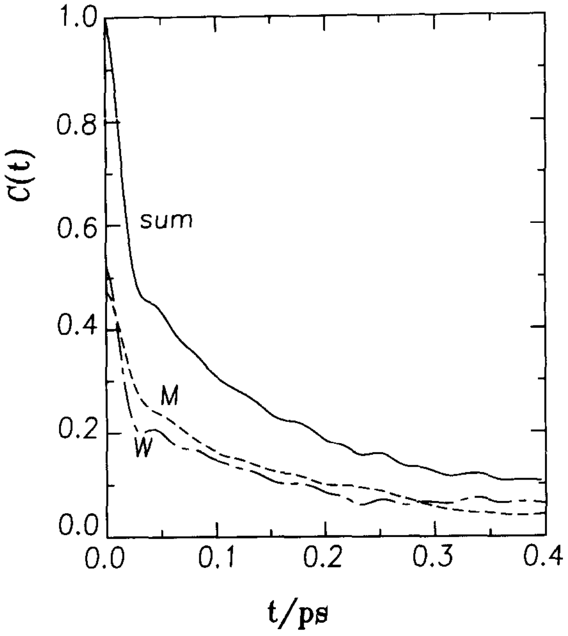

Fig. 4. Same as Fig. 2, but for the small solute.

restoring forces. The data shown in Fig. 2 also indicate that, for this solute, methanol contributes 60% to the total response at $t = 0$. The average equilibrium values of the contributions to ΔE from the two solvents are $\langle \Delta E_{\mathrm{M}} \rangle = -29.4$ kJ mol^{-1} and $\langle \Delta E_{\mathrm{W}} \rangle = -18.8$ kJ mol^{-1}, where $\langle \ldots \rangle$ denotes the equilibrium ensemble average for the system in its initial or final state. (Here these correspond to the same solute–solvent interactions, so the charge state of the solute need not be specified.) These values of the contributions to $\langle \Delta E \rangle$ indicate that this solute is solvated primarily by methanol. This is not surprising, given the large size and, consequently, the low charge density of the interaction-sites of this solute. Water molecules are thus much less electrostatically attracted to it than to other solvent molecules and are largely absent from the first solvation shell. We shall illustrate this below in terms of solute–solvent pair distribution functions.

Before doing that, we examine the behavior of $C(t)$ for the dipole flip of the small solute. Fig. 3 displays the comparison of the response functions for the mixture and pure methanol [15]. As in the large solute case, both curves show the characteristic rapid initial decay, with the mixture relaxing faster than pure methanol. The main differences between the solvation responses for the large (Fig. 1) and small (Fig. 3) solutes are the larger inertial component, and the less pronounced librational oscillations for the smaller solute in both solvents. Fonseca and Ladanyi [15] showed that the early decay of $C(t)$ for this solute in pure methanol was primarily due to the rapid destruction of a solute–solvent H-bond. Judging from the similarity in the mixture response on this time scale, this is the likely cause for the rapid initial decay of the mixture $C(t)$ as well. A closer inspection of Figs. 1 and 3 reveals that at longer times, pure methanol relaxes more slowly in the presence of the small solute, whereas the mixture relaxes more rapidly. We are not yet able to completely explain this behavior, but it is likely be linked to structural differences in the solvation shells surrounding the two types of solutes and the structural changes needed to attain equilibrium solvation.

For the smaller solute, the methanol and water contributions to the total response are shown in Fig. 4. Unlike the solvation of the large solute, both methanol and water contribute approximately equal shares to the $t = 0$ value of

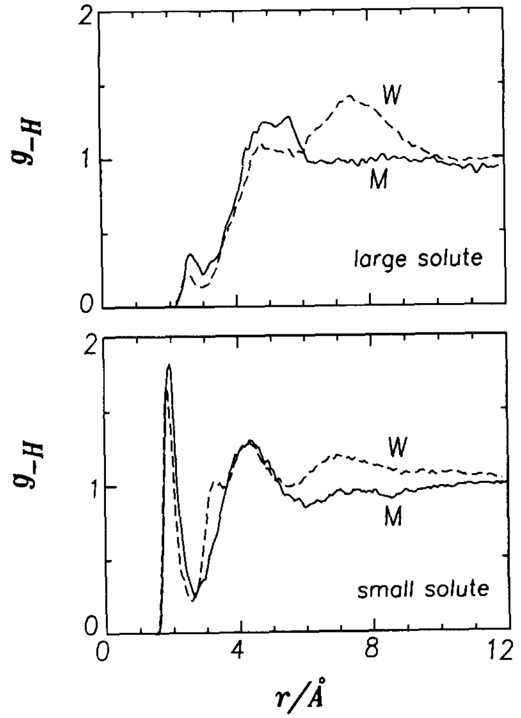

Fig. 5. Solute–solvent site–site pair distribution functions, $g_{-H}(r)$, between the negative solute site and the hydroxy hydrogens of methanol (M, solid line) and water (W, broken line). The results for the large solute are in the top panel and those for the small solute in the bottom panel.

the response, with $C_M(0)$ being slightly smaller than $C_W(0)$. Specifically, the equilibrium excited-ground-state energy gaps are $\langle \Delta E_M \rangle = -53.7$ kJ mol^{-1} and $\langle \Delta E_W \rangle = -59.4$ kJ mol^{-1}. Although there are differences in early decay rates, the time evolution of $C_M(t)$ and $C_W(t)$, shown in Fig. 4, indicate that the methanol and water molecules in the mixture solvate the dipole flip in this solute within similar time scales. As we shall discuss next, the number of water and methanol molecules in the first solvation shell is more nearly equal for this solute than for the larger one, which correlates well with the observed solvation dynamics.

In order to help identify some of the reasons for the differences in the solvation dynamics of the large and small solutes in methanol–water mixtures, we study the average equilibrium distribution of solvent molecules around each solute. This is best accomplished via solute–solvent site–site pair distribution functions, which can be obtained from the equilibrium MD data. We present here a few of these site–site functions. Of course, the temporal evolution of the structure as the system relaxes to equilibrium after the perturbation has been applied [15,16], is also of interest and will be reported elsewhere [17].

The equilibrium pair distribution functions, g_{-H}, between the negative solute site and the hydroxy hydrogens of methanol (M) and water (W) are shown in Fig. 5. The results for the large and small solutes are displayed, respectively, in the top and bottom panels. The results for the large solute exhibit a small first peak at $r = 2.6$ Å. According to geometric criteria for H-bond formation [21,22], a peak at this location corresponds to a solute–solvent H-bond. The small intensity of this peak is a sign that the tendency to form such a bond is low. Indeed, the coordination numbers, obtained from integrating the peaks, are equal to about 0.11, a small number. In contrast, the first peaks of g_{-H} for H_M and H_W with the small solute (bottom panel of Fig. 5) are well defined and much more intense because the smaller solute site diameter allows stronger electrostatic attraction to the H_M and H_W sites. The corresponding coordination numbers are about 0.5 for H_W and 0.6 for H_M. This indicates that this solute is likely to be H-bonded to about one solvent molecule. Dipole flip should lead to a rapid destruction of this bond, consistent with the observed faster initial decay of the responses for the small solute as we have discussed above. Fig. 5 indicates that at longer ranges the H_Ws show more structuring with respect to the negative solute site than do the H_Ms. The implications of this for the dynamics of solvation remain to be investigated.

In Fig. 6, we show the distribution functions between the negatively charged solute site and the methyl group site of methanol, g_{-C}, and between the positive solute site and the oxygen site of water, g_{+O_W}, for the large (upper panel) and small (lower panel) solutes. The curves shown in the upper panel Fig. 6 indicate that the large solute is indeed preferentially solvated by methanol. More specifically, since we know from Fig. 5 that the hydroxy hydrogen is not likely to be close to this site, it is solvated most favorably by the solvent site of lowest charge density. Because of the low charge

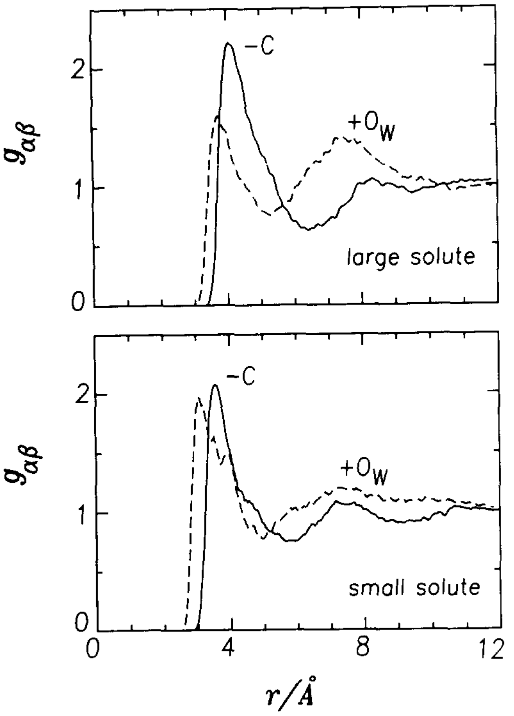

Fig. 6. Site–site pair distribution functions for the solute–solvent pairs −C (solid line), and $+O_W$ (broken line) where C stands for the methyl group of methanol (centered at the carbon atom, and treated as a unit in the H1 model [22]) and O_W for the oxygen site of TIP4P water. The results for the large solute are in the top panel and those for the small solute in the bottom panel.

density of this solute, solvent molecules interact electrostatically less favorably with it than they do with other solvent molecules. The coordination numbers of methanol and water molecules around the large solute sites are approximately 11 and 6, respectively. These numbers were obtained by integrating the first peaks of $g_{-\mathrm{C}}$ and $g_{+\mathrm{O_W}}$ shown in Fig. 6, but similar numbers are obtained from the first peaks of $g_{\alpha\beta}(r)$ functions involving other solute–solvent site pairs like +C, $+\mathrm{O_M}$, etc. Now, for the small solute, for which $g_{-\mathrm{C}}$ and $g_{+\mathrm{O}}$ are shown in the bottom panel of Fig. 6, these pair distributions have nearly equal first peak intensities, with the corresponding coordination numbers being 8.5 for −C and 7 for $+O_W$ site pairs.

Comparing the solute–solvent pair distribution functions associated with the large and small solutes, we conclude that the small solute is surrounded by nearly equal numbers of methanol and water molecules, as would be predicted on the basis of random mixing in an equimolar mixture, whereas the large solute is preferentially solvated by methanol, the less polar of the two cosolvents. Even in the case of the small solute, which shows no preferential solvation, the solvation dynamics is more methanol like than water like. This reflects the fact that the dynamics of the equimolar mixture [22] are closer to the methanol than to the water time scale. Evidently, this will not be the case for solvation in water-rich mixtures [27].

Acknowledgments

This work was supported in part by a grant from the National Science Foundation (USA).

References

[1] P.F. Barbara and W. Jarzeba, Adv. Photochem., 15 (1990) 1.
[2] J.D. Simon, Acc. Chem. Res., 21 (1988) 128.
[3] E.M. Kosower and D. Huppert, Annu. Rev. Phys. Chem., 37 (1986) 127.
[4] H. Heitele, Angew. Chem., Int. Ed. Engl., 32 (1993) 359 .
[5] J.T. Hynes, in J.D. Simon, (Ed.), Ultrafast Spectroscopy, Kluwer, Dordrecht, 1993.
[6] B. Bagchi and A. Chandra, Adv. Chem. Phys., 80 (1991) 1.
[7] M. Maroncelli, J. Mol. Liq., 57 (1993) 1.
[8] M. Rao and B.J. Berne, J. Phys. Chem., 85 (1981) 1498.
[9] M. Maroncelli and G.R. Fleming, J. Chem. Phys., 89 (1988) 5044.
[10] O.A. Karim, A.D.J. Haymet, M.J. Banet and J.D. Simon, J. Phys. Chem., 92 (1988) 3391.
[11] E.A. Carter and J.T. Hynes, J. Chem. Phys., 94 (1991) 5961; J. Phys. Chem., 93 (1989) 2184.
[12] R.M. Levy, D.B. Kitchen, J.T. Blair and K. Krogh-Jespersen, J. Phys. Chem., 94 (1990) 4470.
[13] M. Maroncelli, J. Chem. Phys., 94 (1991) 2084.
[14] T. Fonseca and B.M. Ladanyi, J. Phys. Chem., 95 (1991) 2116.
[15] T. Fonseca and B.M. Ladanyi, J. Mol. Liq., 60 (1993) 1.
[16] D.K. Phelps, M.J. Weaver and B.M. Ladanyi, Chem. Phys., 176 (1993) 575.
[17] K. Ando and S. Kato, J. Chem. Phys., 95 (1991) 5966.
[18] J.S. Bader and D. Chandler, Chem. Phys. Lett., 157 (1989) 501.
[19] M. Maroncelli, P.V. Kumar, A. Papazyan, M.L. Horng, S.J. Rosenthal and G.R. Fleming, in Y. Gauduel and P. Rossky (Eds.) Ultrafast Reaction Dynamics and Solvent Effects, American Institute of Physics Symposium Series, New York, 1993.

[20] A. Declémy, C. Ruillère and P. Kottis, Chem. Phys. Lett., 133 (1987) 447.
A. Declémy and C. Ruillère, in Y. Gauduel and P. Rossky (Eds.), Ultrafast Reaction Dynamics and Solvent Effects, American Institute of Physics Symposium Series, New York, 1993.
J. Yu and M. Berg, Chem. Phys. Lett., 208 (1993) 335.
A.J. Benigno, E. Ahmed and M. Berg, J. Phys. Chem., in press.
[21] B.M. Ladanyi and M.S. Skaf, Annu. Rev. Phys. Chem. 44 (1993) 335.
[22] M. Ferrario, M. Haughney, I.R. McDonald and M.L. Klein, J. Chem. Phys., 93 (1990) 5156.
[23] W.L. Jorgensen, J. Chandrasekhar, R.W. Impey and M.L. Klein, J. Chem. Phys., 79 (1983) 926.
[24] M. Haughney, M. Ferrario and I.R. McDonald, J. Phys. Chem., 91 (1987) 4934.
[25] G. Ciccotti, M. Ferrario and J.P. Ryckaert, Mol. Phys., 47 (1982) 1253.
[26] M.P. Allen and D.J. Tildesley, Computer Simulation of Liquids, Clarendon Press, Oxford, 1987.
[27] M.S. Skaf and B.M. Ladanyi, submitted for publication.